

**Introduction:** Generalized Q-Sampling Imaging (GQI) has recently been introduced by Yeh and colleagues [1], and was shown to have comparable accuracy to other well established q-space methods when it comes to resolving crossing fibres. In addition, this is achievable with as little as 102 points on a grid sampling scheme, bringing the total acquisition time down to a clinically acceptable level. Another advantage of GQI is that it is also applicable to a shell sampling scheme.

Despite their successes in tractography applications, q-space techniques have until now failed to produce scalar metrics that could replace the ones derived from the diffusion tensor model (e.g. mean diffusivity, MD, and fractional anisotropy, FA) in terms of their multi-subject comparability and specificity to pathology. The data acquired with a grid sampling scheme can still be used to estimate a diffusion tensor and respective scalar parameters, but the effects of the high b-values required for q-space imaging (>2000 s/mm<sup>2</sup>) in the accuracy of the resulting DTI-based parameters has not been well characterized. The authors of GQI have also proposed a new scalar metric called quantitative anisotropy (QA), but its properties have not been compared to FA's. In this study we will compare the estimated values of MD, FA and QA0 (first component of QA) obtained with grid and shell sampling schemes, in terms of their precision and ability to differentiate between different brain fibre populations.

**Methods:** Twelve healthy volunteers aged between 18 and 40 were scanned on a 3T scanner (TIM Trio, Siemens), using Siemens advanced diffusion work-in-progress sequence, and STEAM [2] as the diffusion preparation method. The field of view was 240x240mm<sup>2</sup>, matrix size 96x96, and slice thickness 2.5mm (no gap). 55 slices were acquired to achieve full brain coverage, and the voxel resolution was 2.5x2.5x2.5mm<sup>3</sup>. Two sampling schemes were considered: a 102-point grid acquisition with a maximum b-value of 4000 s/mm<sup>2</sup>, and a single shell acquisition using 118 non-collinear gradient directions and a b-value of 1000 s/mm<sup>2</sup>. The two acquisition schemes were matched for total acquisition time (14min 37s), voxel resolution, and bandwidth. FA, MD and QA0 maps were then generated for each acquisition scheme and for the 12 volunteers using dipy (diffusion imaging in python [3]).

All the FA datasets were non-linearly registered into MNI space using fsl tools, and the same transformation parameters were applied to MD and QA0 maps (figure 1 shows the FA and QA0 maps obtained for one volunteer). Fourteen ROIs of different brain regions were drawn in MNI space: putamen (left and right), caudate (left and right), thalamus (left and right), parasagittal white matter (left and right), pons, internal capsule (left and right), and genu, body and splenium of the corpus callosum. Small cubic ROIs were also constructed by finding the centroid of each anatomical ROI and using it as the centre for a 3x3x3 ROI.

For each ROI we calculated the mean value for each metric, and the spatial coefficient of variation (CV) within the ROI (see eq. (1)). The coefficient of variation of each ROI mean across subjects was also calculated, as a measure of each metric's comparability between subjects. The contrast-to-scatter ratio (CSR) (calculated for FA in eq. (2)) is a good measure of a metric's ability to differentiate between different brain fibre populations [4]. Combining the left and right versions of each ROI, we have 9 ROIs of different brain populations, which can be used to define 36 pairs of ROIs, and the CSR of all metrics was calculated for each of these pairs.

Paired t-tests were then conducted to compare the performance of each metric with the two acquisition schemes, and also to compare FA and QA0 directly for each acquisition scheme.

**Results:** The 102 grid sampling scheme produces significantly higher mean FA and QA0 values than the ones obtained with the 118 shell scheme, while the opposite was observed for MD. The CSR results for FA and QA0 were not significantly different between the two acquisition schemes, but the 102 grid scheme produces significantly higher CSRs for MD for 26/36 ROI pairs. For MD, no significant difference was found for the CV across subjects, but for FA and QA0 the 102 scheme produced results more comparable across the different volunteers (figure 3). For FA and MD the 102 scheme showed lower CV within ROIs, especially for white matter, but no difference was found for QA0.

When comparing FA and QA0 directly, our results show that FA produces higher CSRs than QA0 for 23/36 ROI pairs for the 102 grid sampling, and for 19/36 ROI pairs for the 118 shell scheme. FA also shows lower variation across subjects for both acquisition schemes. Finally, FA lower CVs within white matter ROIs, while QA0 shows less variability for grey matter.

The results described and shown above were obtained with the cubic ROIs, but do not differ significantly when the same analysis was applied to larger anatomical ROIs.

**Discussion and Conclusion:** Our results indicate that the MD and FA maps generated from a grid sampling scheme designed for GQI are still suitable for analysis, since they do not show poorer performance when compared to a single shell and low b-value acquisition. In fact, the overall results suggest that the 102 grid sampling produces slightly more robust results than the 118 shell acquisition. A previous study [5] has shown that metrics such as MD and FA benefit from the use of multiple b-values, which could explain the better performance of the 102 grid scheme.

The first component of QA0 shows a good comparability across subjects, which suggests that it could be used for multi-subject comparisons. However, its overall performance was poorer than FA's. In addition, it is important to note that the two acquisition schemes analysed have a total acquisition time higher than a standard acquisition for diffusion tensor imaging analysis (<10 min).

Future work will compare the performance of the grid and shell acquisition schemes in terms of their performance in fibre tracking, and ability to resolve fibre crossings.

**References:** [1] Yeh et al. IEEE TMI 2010. [2] Haase et al. Radiology 160:787-90. [3] <http://nipy.org/dipy> [4] Correia et al. Abstract #3556 ISMRM 09. [5] Correia et al. MRI 27: 163-75.

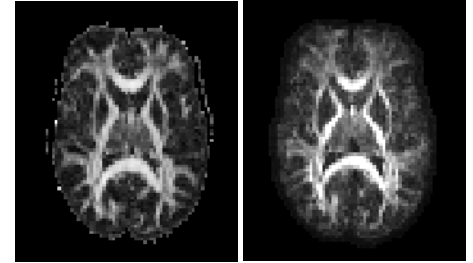


**Figure 1** – FA (left) and QA0 (right) maps for one volunteer with the 102-point

$$CV_{ROI} = \frac{\sigma_x}{\langle x \rangle} = \frac{N_{voxels} \sqrt{\sum_{x_i \in ROI} (x_i - \langle x \rangle)^2}}{\sqrt{N_{voxels} - 1} \sum_{x_i \in ROI} x_i} \quad (1)$$

$$CSR(FA) = \frac{mean(FA)_{ROI1} - mean(FA)_{ROI2}}{\sqrt{var(FA)_{ROI1} + var(FA)_{ROI2}}} \quad (2)$$

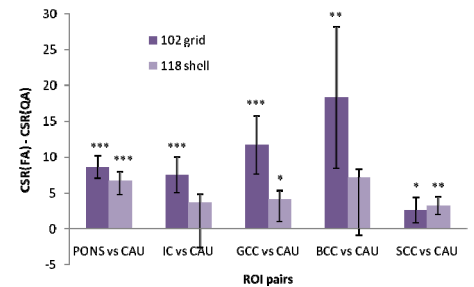


**Figure 2** – Sample results of the paired t-tests comparing CSR(FA) and CSR(QA0).

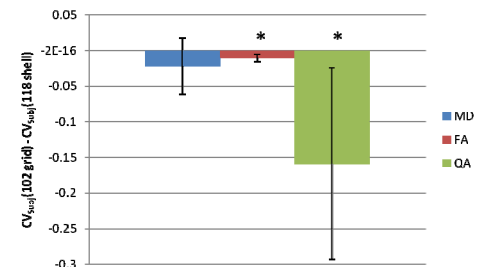


**Figure 3** – Results of the paired t-test comparing the CVs across subjects for MD, FA and QA0.